Iron Oxide-Supported Copper Oxide Nanoparticles (Nanocat-Fe-CuO): Magnetically Recyclable Catalysts for the Synthesis of Pyrazole Derivatives, 4-Methoxyaniline, and Ullmann-type Condensation Reactions

Sharad N. Shelke,*,[†] Swapnil R. Bankar,[†] Ganesh R. Mhaske,[†] Samadhan S. Kadam,[†] Dinesh K. Murade,[†] Shashikant B. Bhorkade,[†] Anuj K. Rathi,[‡] Nenad Bundaleski,[§] Orlando M. N. D. Teodoro,[§] Radek Zboril,[‡] Rajender S. Varma,[⊥] and Manoj B. Gawande*,[‡]

[†]Department of Chemistry, S.S.G.M. College, Kopargaon, Dist. Ahmednagar (MS) 423601, India

[‡]Regional Centre of Advanced Technologies and Materials, Faculty of Science, Department of Physical Chemistry, Palacky University, Šlechtitelů 11, 783 71, Olomouc, Czech Republic

[§]Centre for Physics and Technological Research (CeFITec), Department of Physics, Faculdade de Ciências e Tecnologia, Universidade Nova de Lisboa, 2829-516 Caparica, Portugal

[⊥]Sustainable Technology Division, National Risk Management Research Laboratory, US Environmental Protection Agency, 26 West Martin Luther King Drive, MS 443, Cincinnati, Ohio 45268, United States

Ⓢ *Supporting Information*

ABSTRACT: An efficient and benign protocol is reported for the synthesis of medicinally important pyrazole derivatives, 4-methoxyaniline, and Ullmann-type condensation reaction using magnetically separable and reusable magnetite-supported copper (nanocat-Fe-CuO) nanoparticles under mild conditions. Nanoparticles with average size of 20−30 nm have been synthesized using simple impregnation techniques in aqueous medium from readily available inexpensive starting materials and were recycled six times without loss in catalytic activity.
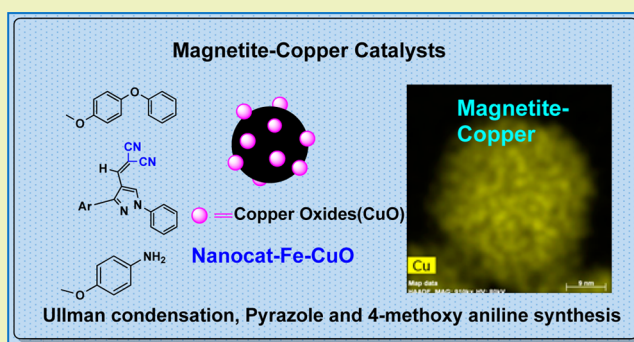
KEYWORDS: *Magnetite-copper oxide, Recyclable catalysts, Pyrazole synthesis, Ullmann reaction, Benign media*

INTRODUCTION

Supported-heterogeneous catalysts are an integral part of catalysis science and technology, and most important organic industrial chemistry relies on them.[1−4] Consequently, it is important to design unique supported catalytic systems for organic transformations and industrially significant reactions; the most recent efforts being the synthesis of metal or metal oxides supported catalysts or nanocatalysts.[5,6] The focus during the past decade has been on nanosupported-metal catalytic processes, and solid platform often deployed on inert supports such as silica, alumina, iron oxides, polymer, and carbon, among others.[7−9] Of these, silica, alumina and especially, inexpensive iron oxides garnered much attention due to their unique characteristics such as high surface area and anchoring possibilities for immobilization.[10,11] Iron oxides, such as magnetite, hematite and some other iron oxides have been well investigated as catalysts or supports in various important organic transformations.[12−17] Magnetite is employed as support for immobilizing catalytic systems such as metals, organoligands, and metal N-heterocyclic carbenes as magnetically recyclable nanocatalysts;[13] such nanocatalysts are

imperative for sustainable organic processes, and hence the drive to design and develop magnetite-supported nanocatalysts. Selected recent examples include an impregnated copper on magnetite in the synthesis of propargylamines[18] and Pd-magnetite for carbonylative Sonogashira coupling reactions;[19,20] copper based catalysts/nanocatalysts are widely employed for various organic processes and catalytic reactions[21−30] including energy conversion.[31−33] Copper and copper oxides nanoparticles often provide the high catalytic activity similar to precious metals with easy availability and low cost. The main drawback of neat metal and metal oxide nanoparticles is their poor recyclability and leaching effects finally leading to decreased yields. To overcome this problem, copper supported catalysts and nanocatalysts are employed in various organic transformation.[34]

Of these, magnetic supported copper catalysts garner special attention as they are robust, inert, and most importantly, can be reused and recycled for several runs without losing their catalytic activity with no/low leaching of copper during the reactions.[35−43]

There are few condensation reactions investigated under mild reaction conditions which use cobalt ferrite nanocatalyst for aldol condensations of aldehydes and ketones,[44] magnetic nanoparticles Fe_3O_4-immobilized domino Knoevenagel condensation, Michael addition, and cyclization catalyst,[45] among some other condensation reactions.[46,47]

Many pyrazole derivatives, especially bearing aryl substituents, have been identified to possess diverse pharmacological activities such as anti-inflammatory, antimicrobial, antihypertensive, etc., including dual anti-inflammatory[48,49] and antimicrobial activity.[50]

In continuation of our efforts to develop greener protocols using nanocatalysis,[51−54] we have developed a simple, and efficient protocol for the synthesis of several pyrazole derivatives, 4-methoxyaniline, and Ullmann-type condensation reaction using nanocat-Fe-CuO MNPs (magnetic nanoparticles); control experiments with unfunctionalized magnetite (without CuO) provided no/low yields in the studied reactions.

■ RESULTS AND DISCUSSION

Nanocat-Fe-CuO MNPs were prepared by the simple wet impregnation method followed by dehydration process[55] (Scheme 1) and well characterized by X-ray diffraction (XRD),

Scheme 1. Synthesis of Nanocat-Fe-CuO MNPs
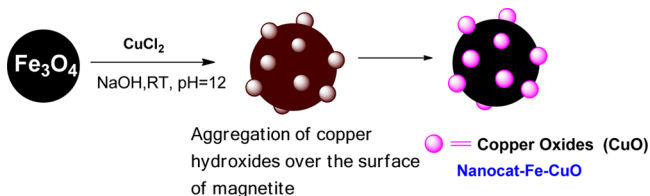
inductive coupled plasma-atomic emission spectroscopy (ICP-AES), transmission electron microscopy (TEM), field-emission gun, scanning electron microscopy, X-ray photoelectron spectroscopy (XPS), electron dispersive spectrometry (FEG-SEM-EDS), and high angle annular dark-field scanning transmission electron microscopy (HAADF-STEM).

The PXRD figure of magnetite and nanocat-Fe-CuO is depicted in Figure 1; the crystallite size of the catalysts was determined by Debye−Scherrer equation was found to be 30.1 nm, which is an agreement with the result obtained from the
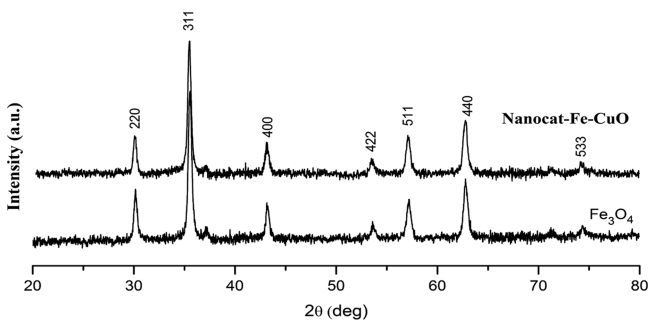

Figure 1. XRD of Fe_3O_4 and nanocat-Fe-CuO.

TEM which shows a size distribution between 20 and 30 nm. The magnetite XRD peaks clearly seen in XRD profile (Figure 1) such as 220, 311, 400, 422, 511 440, and 533 (JCPDS file, no. 19-0629). The weight percentage of Cu was determined to be 4.01% by ICP-AES analysis.

In the survey XPS spectrum of the nanocat-Fe-CuO MNPs the main lines of oxygen, iron, and copper are clearly visible. Additionally, we observed carbon, being a common impurity, and sodium; most likely due to the production process.

The XPS spectrum of the Cu $2p_{3/2}$ line is presented in Figure 2. Broad and intensive satellite peak clearly implies that copper is
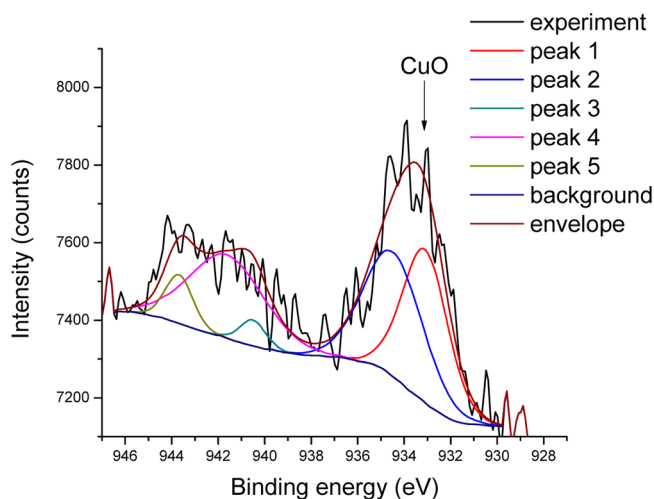

Figure 2. XPS spectrum of Cu $2p_{3/2}$ line taken from the nanocat-Cu-Fe catalyst. The energy axis was corrected to compensate surface charging. The expected Cu $2p_{3/2}$ line position of the peak 1 in the case of CuO is marked by the arrow.

present in the sample as CuO or, eventually $Cu(OH)_2$, while metallic copper or Cu_2O phases can be excluded.[56] At first sight, the position of the peak suggests that copper is present as CuO. The satellite line can be clearly resolved into two contributions, which further supports the assumption that CuO is the dominant copper phase. To confirm that, we performed the line fitting. According to Biesinger and co-workers[56] Cu $2p_{3/2}$ line in CuO can be fitted as a sum of four pseudo-Voigt peak profiles of GL(30) type with well-defined constraints concerning their relative positions and intensities, as well as the widths. When applying those constraints and subtracting the background of Shirley type we obtained very good fit with the peak 1 at 933.1 eV, which perfectly matches its position for CuO.[56]

The TEM image of nanocat-Fe-CuO particles shows that their size is in the range 20−30 nm (Figure 3a), and the EDS image (Figure 3b) exhibits a weak Cu peak, which is consistent with the ICP-AES results.

Figure 4 shows high angle annular dark-field scanning transmission electron microscopy (HAADF-STEM) images of nanocat-Fe-CuO magnetic nanocatalysts. It could be clearly seen from element mapping that the element of Cu, Fe, and O uniformly distributed on the surface of magnetite. The element mapping of C is not shown because a large amount of C exist in the support film of the TEM grid. As depicted in Scheme 1, copper oxide nanoparticles are distributed on the surface of magnetite; it is evidently confirmed by HAADF-STEM images.

In this investigation, we report a convenient and facile method for the Knoevenagel condensation of pyrazole aldehydes with malononitrile and dimedone, which has been carried out in the
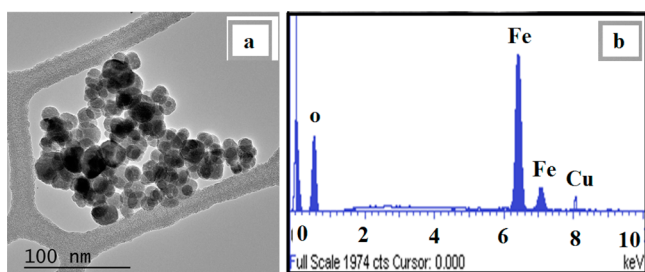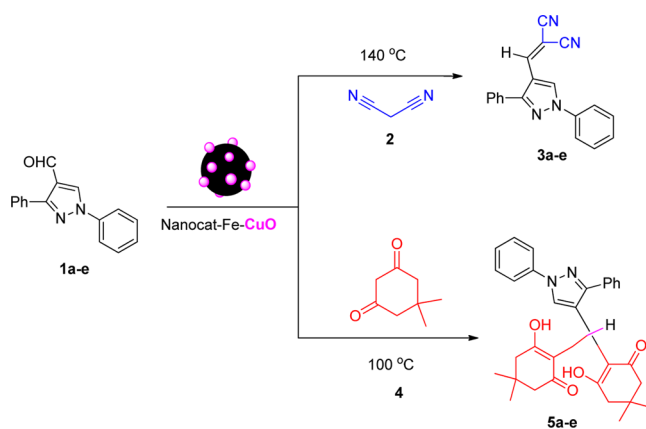
Figure 3. (a) TEM image of nanocat-Fe-CuO at 200 nm. (b) EDS profile nanocat-Fe-CuO.

Scheme 2. Magnetic Nanocat-Fe-CuO Catalyzed Synthesis of Pyrazole Derivatives

presence of nanocat-Fe-CuO as an efficient and green reusable catalyst under solvent-free conditions (Scheme 2). Various substituted 1,3-diphenyl pyrazole aldehydes (**1a−e**) were prepared by Vilsemeier−Haack reaction of the corresponding hydrazone.[57,58]

For optimization of the reaction condition, we have selected the model reaction of 1-phenyl-3-(*p*-tolyl)-1*H*-pyrazole-4-carbaldehyde (**1b**) and malononitrile (**2**) to yield corresponding product (**3b**) (Table 2, entry 2). Initially, we evaluated the reaction under catalyst-free and solvent-free conditions at room temperature, but no product formation was observed (Table 1, entry 1). The same reaction was repeated at 150 °C, and only a trace amount of product was formed (Table 1, entry 2). With nanocat-Fe-CuO (TEM, 20−30 nm) at room temperature, after 24 h, the yield was 35% (Table 1, entry 4), while at 50 °C after 30 min the yield was 58% (Table 1, entry 5) and at 140 °C, after 60 min, the yield was 96% (Table 1, entry 8). CuCl$_2$ precursor did not work for this condensation reaction (Table 1, entries 9, 10).

The substrate scope was further explored for reaction of structurally and electronically diverse aldehydes with malononi-trile and dimedone using magnetite-CuO MNPs under optimized solvent-free conditions (Table 2, entries 1−10).

The reaction of 1,3-diphenyl-1*H*-pyrazole-4-carbaldehyde (**1a**) with malononitrile (**2**) gave 94% yield of the desired product within 1 h (Table 2, entry 1). Pyrazole aldehydes possessing electron-donating and electron-withdrawing groups such as −Cl, −Br, −F, and −CH$_3$ afforded good to excellent yields of the desired products (Table 2, entries 2−6; 8−10). Each experiment was repeated three times to confirm the consistency of the results.

The stability of the catalyst and its catalytic activity was assessed by recycling experiments for the Knoevenagel condensation of pyrazole aldehyde with malononitrile (**2**) in the presence of nanocat-Fe-CuO MNPs under the optimized conditions (Table 2, entry 1). In each cycle, the catalyst was
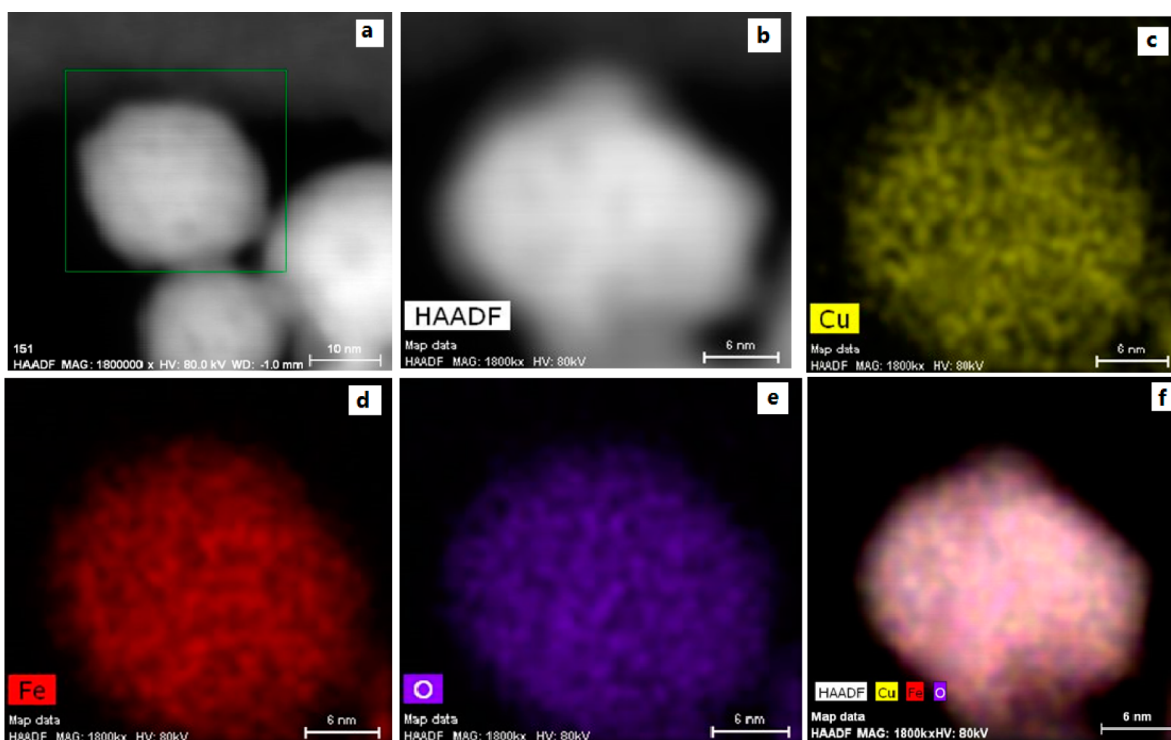
Figure 4. High angle annular dark-field scanning transmission electron microscopy (HAADF-STEM) of nanocat-Fe-CuO. (a) HAADF image of nanocat-Fe-CuO at 10 nm. (b) HAADF image of nanocat-Fe-CuO at 6 nm . (c) HAADF image showing copper. (d) HAADF image showing Fe. (e) HAADF image showing O. (f) HAADF image of showing Cu, Fe, and O together in one nanoparticle of nanocat-Fe-CuO.

Table 1. Optimization of the Reaction[a]

no.	catalysts	solvent	time (h or min)	temp	yield[b] (3b)
1	no catalyst	no solvent	24 (h)	RT	NR
2	no catalyst	no solvent	24 (h)	150 °C	trace
3	nanocat-Fe-CuO	no solvent	30 min	RT	trace
4	nanocat-Fe-CuO	no solvent	24 (h)	RT	35
5	nanocat-Fe-CuO	no solvent	30 min	50 °C	58
6	nanocat-Fe-CuO	no solvent	30 min	100 °C	72
7	nanocat-Fe-CuO	no solvent	30 min	140 °C	81
8	nanocat-Fe-CuO	no solvent	60 min	140 °C	96
9	CuCl$_2$	no solvent	30 min	140 °C	trace
10	CuCl$_2$	no solvent	60 min	140 °C	trace

[a]Reaction conditions: aldehyde = 10 mmol; malononitrile = 12 mmol; nanocat-Fe-CuO = 100 mg; heated in sealed tube. NR = no reaction. [b]Isolated yield.

separated magnetically and washed with ethanol and finally dried at 60 °C under vacuum to remove residual solvents. The results for several cycles are depicted in Figure 5; the yields were 94%, 93%, 91%, 91%, 90%, and 88% from first to sixth cycle; the copper content was found to be 4.01% before reaction and 3.94% after the reaction. We have also done the leaching study of copper metal inside the solution of reaction mixture, and from first to six cycles, we did observe negligible leaching (from 0.01 to 0.02% after each run) and after six cycles, we did observe 0−07% of copper leaching.

The nanocat-Fe-CuO MNPs could be reused up to six times in each of the inspected reactions without any substantial loss of the initial catalytic activity. The additional advantage of the proposed system relates to its ease of separation by means of an external magnet, which could be done at each cycle. Standard leaching experiments (using the hot filtration method and ICP-AES) provided no detectable quantities of Cu in the filtrate, which is a highly catalytic active metal in the reactions. No conversion was observed in the absence of the catalyst (even after 12 h).

To explore the catalytic activity and versatility of nanocat-Fe-CuO catalyst, it was tested for the synthesis of 4-methoxyaniline (**7**) and an Ullmann-type condensation reaction. For the synthesis of 4-methoxyaniline (**7**), the reaction of 4-methoxybromoebenzene with nanocat-Fe-CuO and aqueous ammonia in a mixture of acetone and water was investigated to obtain the corresponding product in quantitative yield (Scheme 3).

Ullmann condensation reaction, involving the reaction of 4-methoxyphenol (**8**) with iodobenzene (**9**) and KOH as a base in DMSO at 120 °C (Scheme 4) afforded the corresponding condensation product in 75% yield within 3 h.

■ EXPERIMENTAL SECTION

Materials and Reagents. All chemicals and reagents were purchased from Sigma-Aldrich and were used as received unless otherwise mentioned. For analytical and preparative thin-layer chromatography, Merck, 0.2 mm and 0.5 mm Kieselgel GF 254 precoated were used, respectively. The spots were visualized using UV light.

Characterization Techniques. The X-ray powder diffraction pattern was obtained using a conventional powder diffractometer RIGAKU, model MiniFlex II benchtop X-ray Diffractometer; X-ray tube Cu Kα (30 kV/15 mA) radiation operating in Bragg−Brentano (θ/2θ)

geometry. (Sample preparation: grinding when needed and compression in the sample holder with a flat glass. The sample area in the sample holder is about 2 cm^2). TEM images were obtained with a Hitachi H8100 microscope, with a ThermoNoran light elements EDS detector and a CCD camera for image acquisition. The nanocat-Fe-CuO fine powder was placed on carbon stub and the images were recorded at 5−15 kV using LFD detector under low vacuum.

SEM images were acquired using a JEOL JSM7001F FEG-SEM. Elemental analysis was performed using a light elements EDS detector from Oxford. The nanocat-Fe-CuO powder was spread on a double-sided carbon tape and analyzed using 25 kV acceleration voltage.

XPS measurement has been performed on a VSW XPS system with the Class 100 energy analyzer being a part of an experimental setup assembled for surface investigation[59] using the nonmonochromatic Mg Kα line (photon energy is 1253.6 eV). Nanocatalyst fine powders were prepared for XPS by pressing on an indium plate as a matrix in order to provide both, mechanical support and electrical contact and analyzed "as received". For the energy axis calibration Ag (110) and polycrystalline Au samples (previously cleaned by ion sputtering) were used. The detailed XPS lines were taken in FAT 22 mode with 0.1 eV of energy step, while the survey spectra was taken in FAT 44 mode with 0.5 eV energy step. The shift of the energy axis due to charging has been determined from the discrepancy of the main contribution of the C 1s peak, assuming it corresponds to adventitious carbon which should be at 284.8 eV surface investigation.[60] The binding energy axis was shifted accordingly for 0.5 eV.

All the recorded melting points were determined on M. P. apparatus model KI-11 (MP-D) and are uncorrected.

Microscopic images were obtained by HRTEM TITAN 60-300 with X-FEG type emission gun, operating at 80 kV. This microscope is equipped with Cs image corrector and a STEM high-angle annular dark-field detector (HAADF). The point resolution is better than 0.08 nm in TEM mode. The elemental mappings were obtained by STEM−energy dispersive X-ray spectroscopy (EDS) with acquisition time 20 min. Sample preparation: The powder samples were dispersed in ethanol and 5 min ultrasonificated. One drop of this solution was placed on a copper grid with holey carbon film. The sample was dried in room temperature.
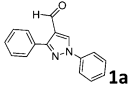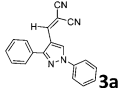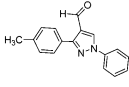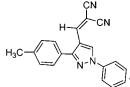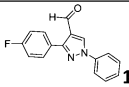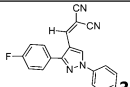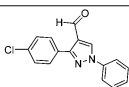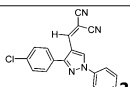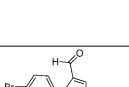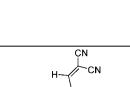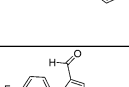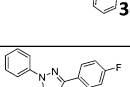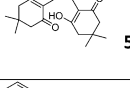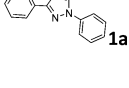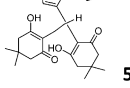
The NMR spectra were recorded on a Bruker 300 MHz (^{1}HNMR) and 75 MHz (^{13}CNMR) instrument using CDCl$_3$ (deuterated chloroform) as a solvent and TMS (tetramethylsilane) as an internal standard; the chemical shifts (δ) are reported in ppm (part(s) per million) and coupling constants (J) are given in Hertz. Signal multiplicities are represented by s (singlet), d (doublet), t (triplet), dd (double doublet), and m (multiplet). TLC was performed on precoated silica gel glass plates (Kieselgel 60, 254, E. Merck, Germany).

Preparation of Fe$_3$O$_4$ MNPs. FeCl$_3$·6H$_2$O (5.4 g) and urea (3.6 g) were dissolved in water (200 mL) at 85 to 90 °C for 2 h. To the ensuing brown reaction mixture, cooled to room temperature, was added FeSO$_4$·7H$_2$O (2.8 g) and then 0.1 M NaOH until pH 10. The molar ratio of Fe(III) to Fe(II) in the above system was nearly 2.00. The resultant hydroxides were treated by ultrasound in the sealed flask at 30 to 35 °C for 30 min. After aging for 5 h, the obtained black powder (Fe$_3$O$_4$) was washed, and dried under vacuum.

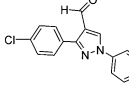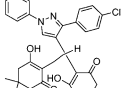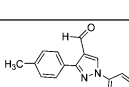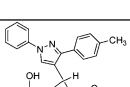**Preparation of the Nanocat-Fe-CuO Catalyst.** Magnetite nanoparticles, Fe$_3$O$_4$ (2 g), and copper chloride (CuCl$_2$·2H$_2$O, for 5 wt % of Cu on magnetite) were stirred at room temperature in aqueous solution (50 mL) for 1 h. After impregnation, the suspension was adjusted to pH 12−13 by adding sodium hydroxide (1.0 M) and further stirred for 20 h. The solid was washed with distilled water (5 × 10 mL), and the resulting nanocat-Fe-CuO particles were sonicated for 10 min, washed with distilled water and subsequently with ethanol, and dried under vacuum at 60 °C for 24 h. The Cu content was found to be 4.01% as determined by ICP-AES.

General Procedure for the Synthesis of Pyrazole Derivatives (3a−3e). A stoichiometric mixture of various substituted pyrazole aldehydes **1a−e** (10 mmol) with malononitrile **2** (10 mmol) was melted under pressurized sealed tube containing nanocat-Fe-CuO (100 mg, 0.5 mol %) by heating at 140 °C for 50−70 min. At room temperature the progress of the reaction, monitored by TLC, and no product was obtained after 24h. After completion of the reaction mixture, the MNPs

Table 2. Solvent-free Knoevenagel Condensation Reactions Catalyzed by Nanocat-Fe-CuO[a]

Entry	Reactant	Time (min.)	Products	Yield[b] (%)
1	**1a**	60	**3a**	94
2	**1b**	60	**3b**	96
3	**1c**	70	**3c**	87
4	**1d**	50	**3d**	88
5	**1e**	64	**3e**	84
6	**1c**	70	**5a**	94
7	**1a**	60	**5b**	98
8	**1d**	60	**5c**	87
9	**1b**	60	**5d**	96
10	**1e**	60	**5e**	91

[a]Reaction conditions: aldehyde = 10 mmol; malononitrile = 10 mmol or dimedone = 20 mmol); nanocat-Fe-CuO = 100 mg, 0.5 mol %; temperature = 140 °C for 50−70 min. [b]Isolated yield.

were separated by magnetic decantation. The products were obtained in quantitative yields, after drying at 100 °C in a vacuum Rota-vapor without further purification.

This typical experimental procedure was followed to prepare other analogues of this series. The compounds synthesized by above procedures are listed in Table 2 with their characterization data.

3a. ^{1}H NMR (300 MHz, CDCl$_3$,δ, pm): 7.26−7.81 (11H, m, HAr), 9.06 (1H, s, −CH=C(CN)$_2$). ^{13}C NMR (75 MHz, CDCl$_3$): 156.3,

151.1, 138.5, 130.1, 129.8, 129.29, 129.2, 129.2, 128.6, 120.0, 115.0, 113.9, 113.9.

3b. ^{1}H NMR (300 MHz, CDCl$_3$, δ, ppm): 2.46 (3H, s, −CH$_3$), 7.27−7.83 (10H, m, HAr), 9.05 (1H, s, −CH=C(CN)$_2$). ^{13}C NMR (75 MHz, CDCl$_3$): 155.3, 150.7, 131.1, 131.0, 129.8, 129.3, 128.7, 120.0, 116.5, 116.2, 114.9.

3c. ^{1}H NMR (300 MHz, CDCl$_3$, δ, ppm): 1.63 (3H, s, −CH$_3$), 7.22−7.81 (9H, m, HAr), 9.04 (1H, s, −CH=C(CN)$_2$). ^{13}C NMR (75 MHz,

1703

dx.doi.org/10.1021/sc500160f | ACS Sustainable Chem. Eng. 2014, 2, 1699−1706
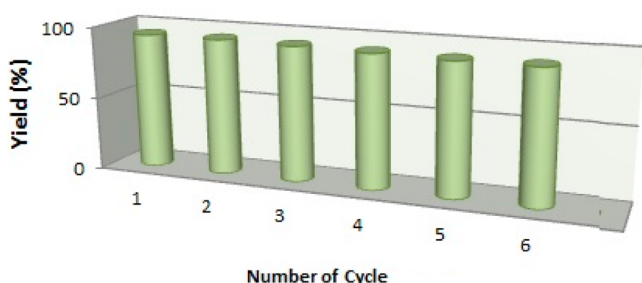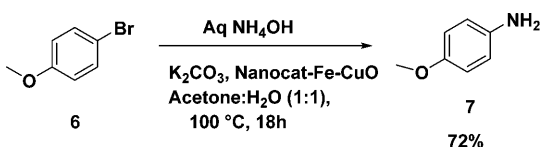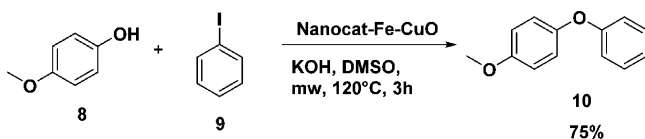
Reusability of nanocat-Fe-CuO

Figure 5. Recyclability of nanocat-Fe-CuO.

Scheme 3. Synthesis of 4-Methoxyaniline

Scheme 4. Nanocat-Fe-CuO Catalyzed Ullmann Condensation Reaction of 4-Methoxyphenol (8) with Iodobenzene (9)

CDCl$_3$): 165.5, 155.3, 150.7, 138.5, 131.1, 129.8, 129.3, 128.7, 120.0, 116.5, 116.2, 114.9, 113.8, 108.7.

3d. ^{1}H NMR (300 MHz, CDCl$_3$, δ, ppm): 7.49—8.23 (10H, m, HAr), 9.2 (1H, s, −CH═C(CN)$_2$). ^{13}C NMR (75 MHz, CDCl$_3$): 154.1, 152.8, 150.0, 144.5, 139.7, 138.7, 134.8, 131.2, 130.8, 130.3, 129.5, 128.8, 120.3, 115.0, 114.1, 112.5, 97.0, 93.8, 85.0.

3e. ^{1}H NMR (300 MHz, CDCl$_3$, δ, ppm): 7.19—7.72 (10H, m, HAr), 8.98 (1H, s, −CH═C(CN)$_2$). ^{13}C NMR (75 MHz, CDCl$_3$): 155.1, 150.5, 138.4, 132.4, 130.6, 129.9, 129.4, 129.0, 128.8, 124.5, 120.1, 114.8, 113.7.

General Procedure for the Synthesis of Compounds 5a−5e. Pressurized seal tube was charged with various substituted pyrazole aldehydes **1a−e** (10 mmol) and dimedone **4** (20 mmol) with nanocat-Fe-CuO. The reaction mixture was heated at 100 °C for 60 min. After completion of the reaction mixture, the magnetic nano particles were separated by magnetic decantation. Quantitative yields of the products were obtained, after drying at 100 °C in vacuum Rota-vapor.

The formation of compounds **5a−e** was confirmed by m.p., mixed m.p., and spectral studies. This typical experimental procedure was followed to prepare other analogues of this series. The compounds synthesized by above procedures are listed in Table 2 with their characterization data.

5a. ^{1}H NMR (300 MHz, CDCl$_3$, δ, ppm): 0.98 (12H, s, −CH$_3$), 2.07 (4H, s, −CH$_2$), 2.15 (4H, s, −CH$_2$), 4.79 (1H, s, methine), 6.78−7.78 (10H, m, HAr), 12.01 (2H, s, −OH). ^{13}C NMR (75 MHz, CDCl$_3$): 196.6, 189.8, 164.2, 161.9, 160.9, 151.3, 139.9, 130.9, 130.8, 130.6, 129.2, 127.3, 126.1, 124.9, 118.8, 50.7, 40.8, 32.0, 28.5, 28.1.

5b. ^{1}H NMR (300 MHz, CDCl$_3$, δ, ppm): 0.94 (12H, s, −CH$_3$), 1.93 (4H, s, −CH$_2$), 2.12 (4H, s, −CH$_2$), 5.66 (1H, s, methine), 7.22−7.67 (11H, m, HAr), 12.11 (2H, s, −OH). ^{13}C NMR (75 MHz, CDCl$_3$): 189.3, 164.2, 161.9, 160.0, 151.3, 139.9, 130.9, 130.8, 130.6, 129.2, 127.3, 126.1, 124.9, 118.8, 115.2, 115.1, 114.1, 46.8, 46.2, 31.7, 28.3, 28.0.

5c. ^{1}H NMR (300 MHz, CDCl$_3$, δ, ppm): 1.02 (12H, s, −CH$_3$), 1.95 (4H, s, −CH$_2$), 2.20 (4H, s, −CH$_2$), 5.66 (1H, s, methine), 7.22−7.67 (10H, m, HAr), 12.09 (2H, s, −OH). ^{13}C NMR (75 MHz, CDCl$_3$):

203.7, 189.8, 150.1, 139.8, 133.7, 132.5, 130.9, 130.4, 129.8, 129.3, 129.1, 128.1, 127.2, 126.3, 119.9, 50.7, 46.3, 40.8, 32.0, 30.9.

5d. ^{1}H NMR (300 MHz, CDCl$_3$, δ, ppm): 0.98 (12H, s, −CH$_3$), 2.03 (4H, s, −CH$_2$), 2.09 (4H, s, −CH$_2$), 2.37 (3H, s, CH$_3$Ar), 5.64 (1H, s, methine), 7.16−7.67 (10H, m, HAr), 12.11 (2H, s, −OH). ^{13}C NMR (75 MHz, CDCl$_3$): 196.5, 189.2, 161.8, 151.5, 140.1, 137.3, 131.1, 129.2, 128.6, 128.4, 127.8, 126.8, 126.0, 118.9, 117.9, 50.7, 46.2, 40.8, 28.3, 28.1.

5e. ^{1}H NMR (300 MHz, CDCl$_3$, δ, ppm): 1.04 (12H, s, −CH$_3$), 2.07 (4H, s, −CH$_2$), 2.17 (4H, s, −CH$_2$), 5.63 (1H, s, methine), 7.26−7.80 (10H, m, HAr), 12.07 (2H, s, −OH). ^{13}C NMR (75 MHz, CDCl$_3$): 189.3, 150.1, 139.9, 133.0, 131.1, 130.1, 129.3, 127.2, 126.3, 121.8, 119.0, 118.1, 115.6, 100.0, 46.8, 46.2, 31.6, 28.1, 25.6.

Synthesis of 4-Methoxyaniline (7). To a stirred solution of 4-bromo anisole **6** (100 mg, 0.534 mmol) and potassium carbonate (147 mg, 1.06 mmol) in acetone: water 1:1 (1.5 mL), nanocat-Fe-CuO catalyst (100 mg) was added followed by aq. NH$_4$OH (2 mL). The resulting mixture was stirred at 100 °C for 18 h. The progress of the reaction was monitored by TLC, after consumption of starting material; reaction mixture was diluted with water and extracted with ethyl acetate (3 × 40 mL). The combined organic layer was dried over anhydrous sodium sulfate and concentrated under reduced pressure to afford the corresponding products (**7**) in 72% yield after purification.

Synthesis of 1-Methoxy-4-phenoxybenzene (10). To a stirred solution of iodobenzene (**9**) (204 mg, 1 mmol) and 4-methoxy phenol (**8**) (124 mg, 1 mmol) in DMSO (2 mL) were added nanocat-Fe-CuO catalyst (160 mg) and KOH (112 mg, 2 mmol). The resulting mixture was stirred at 120 °C for 3 h in microwave. The progress of reaction was monitored by TLC, after consumption of starting material; reaction mixture was diluted with water and extracted with ether (3 × 40 mL). The combined organic layers were dried over anhydrous sodium sulfate and concentrated under reduced pressure to produce crude material which was subjected to column chromatography on silica gel (100−200 mesh size) with 0−5% EtOAc/hexane to get 1-methoxy-4-phenoxybenzene product (**10**) in 75% yield.

■ CONCLUSIONS

An active and versatile nanocat-Fe-CuO catalyst was prepared from inexpensive precursors using a simple impregnation method and was found to be highly efficient in the synthesis of 4-methoxyaniline, pyrazole derivatives, and Ullmann-type condensation. The magnetically separable nanocat-Fe-CuO was found to be stable and displayed its initial catalytic activity even after six runs in all the investigated reactions. The simple procedure, mild reaction conditions, economic feasibility, and good to excellent product yields, renders this an attractive sustainable option. Further applicability of this catalyst for other reactions is under investigation in our laboratories.

■ ASSOCIATED CONTENT

ⓢ Supporting Information

General methods. This material is available free of charge via the Internet at http://pubs.acs.org.

■ AUTHOR INFORMATION

Corresponding Authors

*Tel.: +91-8888199853. E-mail: snshelke@yahoo.co.in (S.N.S.).
*E-mail: manoj.gawande@upol.cz ; mbgawande@yahoo.co.in (M.B.G.).

Notes

The authors declare no competing financial interest.

■ REFERENCES

(1) Astruc, D.; Lu, F.; Aranzaes, J. R. Nanoparticles as recyclable catalysts: The frontier between homogeneous and heterogeneous catalysis. *Angew. Chem., Int. Ed.* **2005**, *44* (48), 7852−7872.

(2) Gawande, M. B.; Pandey, R. K.; Jayaram, R. V. Role of mixed metal oxides in catalysis science-versatile applications in organic synthesis. *Catal. Sci. Technol.* **2012**, *2* (6), 1113−1125.

(3) Corma, A.; Garcia, H. Supported gold nanoparticles as catalysts for organic reactions. *Chem. Soc. Rev.* **2008**, *37* (9), 2096−2126.

(4) Climent, M. J.; Corma, A.; Iborra, S. Heterogeneous Catalysts for the One-Pot Synthesis of Chemicals and Fine Chemicals. *Chem. Rev.* **2011**, *111* (2), 1072−1133.

(5) Gawande, M. B.; Branco, P. S.; Parghi, K.; Shrikhande, J. J.; Pandey, R. K.; Ghumman, C. A. A.; Bundaleski, N.; Teodoro, O.; Jayaram, R. V. Synthesis and characterization of versatile MgO-ZrO2 mixed metal oxide nanoparticles and their applications. *Catal. Sci. Technol.* **2011**, *1* (9), 1653−1664.

(6) Gawande, M. B.; Shelke, S. N.; Branco, P. S.; Rathi, A.; Pandey, R. K. Mixed metal MgO−ZrO$_2$ nanoparticle-catalyzed O-tert-Boc protection of alcohols and phenols under solvent-free conditions. *Appl. Organomet. Chem.* **2012**, *26* (8), 395−400.

(7) Gawande, M. B.; Rathi, A.; Nogueira, I. D.; Ghumman, C. A. A.; Bundaleski, N.; Teodoro, O. M. N. D.; Branco, P. S. A Recyclable Ferrite−Co Magnetic Nanocatalyst for the Oxidation of Alcohols to Carbonyl Compounds. *ChemPlusChem.* **2012**, *2012* (77), 865−871.

(8) Kim, S. B.; Pike, R. D.; Sweigart, D. A. Multifunctionality of Organometallic Quinonoid Metal Complexes: Surface Chemistry, Coordination Polymers, and Catalysts. *Acc. Chem. Res.* **2013**, *46* (11), 2485−2497.

(9) Lu, J.; Toy, P. H. Organic Polymer Supports for Synthesis and for Reagent and Catalyst Immobilization. *Chem. Rev.* **2009**, *109* (2), 815−838.

(10) Guo, H.; Liu, X.; Xie, Q.; Wang, L.; Peng, D.-L.; Branco, P. S.; Gawande, M. B. Disproportionation route to monodispersed copper nanoparticles for the catalytic synthesis of propargylamines. *Rsc. Adv.* **2013**, *3* (43), 19812−19815.

(11) Suzuta, T.; Toba, M.; Abe, Y.; Yoshimura, Y. Iron Oxide Catalysts Supported on Porous Silica for the Production of Biodiesel from Crude Jatropha Oil. *J. Am. Oil Chem. Soc.* **2012**, *89* (11), 1981−1989.

(12) Kale, S. R.; Kahandal, S. S.; Gawande, M. B.; Jayaram, R. V. Magnetically recyclable [gamma]-Fe2O3-HAP nanoparticles for the cycloaddition reaction of alkynes, halides and azides in aqueous media. *Rsc. Adv.* **2013**, *3* (22), 8184−8192.

(13) Gawande, M. B.; Branco, P. S.; Varma, R. S. Nano-magnetite (Fe$_3$O$_4$) as a support for recyclable catalysts in the development of sustainable methodologies. *Chem. Soc. Rev.* **2013**, *42* (8), 3371−3393.

(14) Baig, R. B. N.; Varma, R. S. A highly active and magnetically retrievable nanoferrite-DOPA-copper catalyst for the coupling of thiophenols with aryl halides. *Chem. Commun.* **2012**, *48* (20), 2582−2584.

(15) Vaddula, B. R.; Saha, A.; Leazer, J.; Varma, R. S. A simple and facile Heck-type arylation of alkenes with diaryliodonium salts using magnetically recoverable Pd-catalyst. *Green Chem.* **2012**, *14* (8), 2133−2136.

(16) Rezaeifard, A.; Jafarpour, M.; Farshid, P.; Naeimi, A. Nano-magnet-Supported Partially Brominated Manganese-Porphyrin as a Promising Catalyst for the Selective Heterogeneous Oxidation of

(17) Li, P.-H.; Li, B.-L.; An, Z.-M.; Mo, L.-P.; Cui, Z.-S.; Zhang, Z.-H. Magnetic Nanoparticles (CoFe$_2$O$_4$)-Supported Phosphomolybdate as an Efficient, Green, Recyclable Catalyst for Synthesis of *β*-Hydroxy Hydroperoxides. *Adv. Synth. Catal.* **2013**, *355* (14−15), 2952−2959.

(18) Aliaga, M. J.; Ramon, D. J.; Yus, M. Impregnated copper on magnetite: an efficient and green catalyst for the multicomponent preparation of propargylamines under solvent free conditions. *Org. Biomol. Chem.* **2010**, *8* (1), 43−46.

(19) Liu, J. M.; Peng, X. G.; Sun, W.; Zhao, Y. W.; Xia, C. G. Magnetically separable Pd catalyst for carbonylative Sonogashira coupling reactions for the synthesis of alpha,*β*-alkynyl ketones. *Org. Lett.* **2008**, *10* (18), 3933−3936.

(20) Ranganath, K. V. S.; Kloesges, J.; Schafer, A. H.; Glorius, F. Asymmetric Nanocatalysis: N-Heterocyclic Carbenes as Chiral Modifiers of Fe$_3$O$_4$/Pd nanoparticles. *Angew. Chem., Int. Ed.* **2010**, *49* (42), 7786−7789.

(21) Sharghi, H.; Khalifeh, R.; Doroodmand, M. M. Copper nanoparticles on charcoal for multicomponent catalytic synthesis of 1,2,3-triazole derivatives from benzyl halides or alkyl halides, terminal alkynes and sodium azide in water as a "green" solvent. *Adv. Synth. Catal.* **2009**, *351* (1 + 2), 207−218.

(22) Alonso, F.; Moglie, Y.; Radivoy, G.; Yus, M. Multicomponent synthesis of 1,2,3-triazoles in water catalyzed by copper nanoparticles on activated carbon. *Adv. Synth. Catal.* **2010**, *352* (18), 3208−3214.

(23) Ranu, B. C.; Dey, R.; Chatterjee, T.; Ahammed, S. Copper nanoparticle-catalyzed carbon-carbon and carbon-heteroatom bond formation with a greener perspective. *ChemSusChem.* **2012**, *5* (1), 22−44.

(24) Alonso, F.; Moglie, Y.; Radivoy, G.; Yus, M. Multicomponent Click Synthesis of 1,2,3-Triazoles from Epoxides in Water Catalyzed by Copper Nanoparticles on Activated Carbon. *J. Org. Chem.* **2011**, *76* (20), 8394−8405.

(25) Mitsudome, T.; Mikami, Y.; Ebata, K.; Mizugaki, T.; Jitsukawa, K.; Kaneda, K. Copper nanoparticles on hydrotalcite as a heterogeneous catalyst for oxidant-free dehydrogenation of alcohols. *Chem. Commun.* **2008**, *39*, 4804−4806.

(26) Wang, K.; Bi, X. H.; Xing, S. X.; Liao, P. Q.; Fang, Z. X.; Meng, X. Y.; Zhang, Q. A.; Liu, Q.; Ji, Y. Cu$_2$O acting as a robust catalyst in Cu AAC reactions: water is the required medium. *Green Chem.* **2011**, *13* (3), 562−565.

(27) Alonso, F.; Moglie, Y.; Radivoy, G.; Yus, M. Copper-Catalyzed Multicomponent Click Synthesis of 5-Alkynyl 1,2,3-Triazoles under Ambient Conditions. *Synlett.* **2012**, *15*, 2179−2182.

(28) Strassberger, Z.; Alberts, A. H.; Louwerse, M. J.; Tanase, S.; Rothenberg, G. Catalytic cleavage of lignin [small beta]-O-4 link mimics using copper on alumina and magnesia-alumina. *Green Chem.* **2013**, *15* (3), 768−774.

(29) Kou, J.; Saha, A.; Bennett-Stamper, C.; Varma, R. S. Inside-out core-shell architecture: controllable fabrication of Cu$_2$O@Cu with high activity for the Sonogashira coupling reaction. *Chem. Commun.* **2012**, *48* (47), 5862−5864.

(30) Ranu, B. C.; Dey, R.; Chatterjee, T.; Ahammed, S. Copper Nanoparticle-Catalyzed Carbon-Carbon and Carbon-Heteroatom Bond Formation with a Greener Perspective. *ChemSusChem.* **2012**, *5* (1), 22−44.

(31) Boettcher, S. W.; Spurgeon, J. M.; Putnam, M. C.; Warren, E. L.; Turner-Evans, D. B.; Kelzenberg, M. D.; Maiolo, J. R.; Atwater, H. A.; Lewis, N. S. Energy-Conversion Properties of Vapor-Liquid-Solid-Grown Silicon Wire-Array. *Photocath. Sci.* **2010**, *327* (5962), 185−187.

(32) Takagi, D.; Homma, Y.; Hibino, H.; Suzuki, S.; Kobayashi, Y. Single-walled carbon nanotube growth from highly activated metal nanoparticles. *Nano Lett.* **2006**, *6* (12), 2642−2645.

(33) Vitulli, G.; Bernini, M.; Bertozzi, S.; Pitzalis, E.; Salvadori, P.; Coluccia, S.; Martra, G. Nanoscale Copper Particles Derived from Solvated Cu Atoms in the Activation of Molecular. *Oxygen. Chem. Mater.* **2002**, *14* (3), 1183−1186.

(34) Kamal, A.; Srinivasulu, V.; Murty, J. N. S. R. C.; Shankaraiah, N.; Nagesh, N.; Srinivasa Reddy, T.; Subba Rao, A. V. Copper Oxide Nanoparticles Supported on Graphene Oxide- Catalyzed S-Arylation: An Efficient and Ligand-Free Synthesis of Aryl Sulfides. *Adv. Synth. Catal.* **2013**, *355* (11−12), 2297−2307.

(35) Zhang, R.; Liu, J.; Wang, S.; Niu, J.; Xia, C.; Sun, W. Magnetic CuFe$_2$O$_4$ Nanoparticles as an Efficient Catalyst for C-O Cross-Coupling of Phenols with Aryl Halides. *ChemCatChem.* **2011**, *3* (1), 146−149.

(36) Swapna, K.; Murthy, S. N.; Jyothi, M. T.; Nageswar, Y. V. D. Nano-CuFe$_2$O$_4$ as a magnetically separable and reusable catalyst for the synthesis of diaryl/aryl alkyl sulfides via cross-coupling process under ligand-free conditions. *Org. Biomol. Chem.* **2011**, *9* (17), 5989−5996.

(37) Swapna, K.; Murthy, S. N.; Nageswar, Y. V. D. Magnetically Separable and Reusable Copper Ferrite Nanoparticles for Cross-Coupling of Aryl Halides with Diphenyl Diselenide. *Eur. J. Org. Chem.* **2011**, *10*, 1940−1946.

(38) Ishikawa, S.; Hudson, R.; Moores, A.; Li, C. J. Ligand Modified CuFe$_2$O$_4$ Nanoparticles as Magnetically Recoverable and Reusable Catalyst for Azide-Alkyne Click Condensation. *Heterocycles* **2012**, *86* (2), 1023−1030.

(39) Kumar, B.; Reddy, K. H. V.; Madhav, B.; Ramesh, K.; Nageswar, Y. V. D. Magnetically separable CuFe$_2$O$_4$ nano particles catalyzed multicomponent synthesis of 1,4-disubstituted 1,2,3-triazoles in tap water using 'click chemistry'. *Tetrahedron Lett.* **2012**, *53* (34), 4595−4599.

(40) Hudson, R.; Ishikawa, S.; Li, C. J.; Moores, A. Magnetically Recoverable CuFe$_2$O$_4$ Nanoparticles as Highly Active Catalysts for Csp(3)-Csp and Csp(3)-Csp(3) Oxidative Cross-Dehydrogenative Coupling. *Synlett* **2013**, *24* (13), 1637−1642.

(41) Hudson, R.; Li, C. J.; Moores, A. Magnetic copper-iron nanoparticles as simple heterogeneous catalysts for the azide-alkyne click reaction in water. *Green Chem.* **2012**, *14* (3), 622−624.

(42) Kantam, M. L.; Yadav, J.; Laha, S.; Jha, S. Synthesis of Propargylamines by Three-Component Coupling of Aldehydes, Amines and Alkynes Catalyzed by Magnetically Separable Copper Ferrite Nanoparticles. *Synlett* **2009**, *11*, 1791−1794.

(43) Kasi Viswanath, I. V.; Murthy, Y. L. N. One-Pot, Three-Component Synthesis of 1, 4-Dihydropyridines by Using Nano Crystalline Copper Ferrite. *Chem. Sci. Trans.* **2013**, *2* (1), 227−233.

(44) Senapati, K. M.; Phukan, P. Magnetically separable cobalt ferrite nanocatalyst for aldol condensations of aldehydes and ketones. *Bull. Catal. Soc. Indian* **2011**, *9*, 1−8.

(45) Rostami, A.; Atashkar, B.; Gholami, H. Novel magnetic nanoparticles Fe$_3$O$_4$-immobilized domino Knoevenagel condensation, Michael addition, and cyclization catalyst. *Catal. Commun.* **2013**, *37*, 69−74.

(46) Banon-Caballero, A.; Guillena, G.; Najera, C.; Faggi, E.; Sebastian, R. M.; Vallribera, A. Recoverable silica-gel supported binam-prolinamides as organocatalysts for the enantioselective solvent-free intra- and intermolecular aldol reaction. *Tetrahedron* **2013**, *69* (4), 1307−1315.

(47) Kandel, K.; Althaus, S. M.; Peeraphatdit, C.; Kobayashi, T.; Trewyn, B. G.; Pruski, M. Slowing, II. Substrate inhibition in the heterogeneous catalyzed aldol condensation: A mechanistic study of supported organocatalysts. *J. Catal.* **2012**, *291*, 63−68.

(48) Bekhit, A. A.; Fahmy, H. T. Y.; Rostom, S. A. F.; Bekhit, A. E.-D. A. Synthesis and biological evaluation of some thiazolylpyrazole derivatives as dual anti-inflammatory antimicrobial agents. *Eur. J. Med. Chem.* **2010**, *45* (12), 6027−6038.

(49) Bekhit, A. A.; Hymete, A.; Bekhit, A. E.-D. A.; Damtew, A.; Aboul-Enein, H. Y. Pyrazoles as Promising Scaffold for the Synthesis of Anti-Inflammatory and/or Antimicrobial Agent: A Review. *Mini-Rev. Med. Chem.* **2010**, *10* (11), 1014−1033.

(50) Vijesh, A. M.; Isloor, A. M.; Shetty, P.; Sundershan, S.; Fun, H. K. New pyrazole derivatives containing 1,2,4-triazoles and benzoxazoles as potent antimicrobial and analgesic agents. *Eur. J. Med. Chem.* **2013**, *62*, 410−415.

(51) Gawande, M. B.; Bonifacio, V. D. B.; Luque, R.; Branco, P. S.; Varma, R. S. Benign by design: catalyst-free in-water, on-water green chemical methodologies in organic synthesis. *Chem. Soc. Rev.* **2013**, *42* (12), 5522−5551.

(52) Gawande, M. B.; Rathi, A. K.; Nogueira, I. D.; Varma, R. S.; Branco, P. S. Magnetite-supported sulfonic acid: a retrievable nano-catalyst for the Ritter reaction and multicomponent reactions. *Green Chem.* **2013**, *15* (7), 1895−1899.

(53) Gawande, M. B.; Bonifácio, V. D. B.; Luque, R.; Branco, P. S.; Varma, R. S. Solvent-Free and Catalysts-Free Chemistry: A Benign Pathway to Sustainability. *ChemSusChem.* **2014**, *7* (1), 24−44.

(54) Gawande, M. B.; Shelke, S. N.; Zboril, R.; Varma, R. S. Microwave-Assisted Chemistry: Synthetic Applications for Rapid Assembly of Nanomaterials and Organics. *Acc. Chem. Res.* **2014**, *47* (4), 1338−1348.

(55) Gawande, M. B.; Bonifacio, V. D. B.; Varma, R. S.; Nogueira, I. D.; Bundaleski, N.; Ghumman, C. A. A.; Teodoro, O. M. N. D.; Branco, P. S. Magnetically recyclable magnetite-ceria (Nanocat-Fe-Ce) nanocatalyst - applications in multicomponent reactions under benign conditions. *Green Chem.* **2013**, *15*, 1226−1231.

(56) Biesinger, M. C.; Lau, L. W. M.; Gerson, A. R.; Smart, R. S. C. Resolving surface chemical states in XPS analysis of first row transition metals, oxides and hydroxides: Sc, Ti, V, Cu and Zn. *Appl. Surf. Sci.* **2010**, *257* (3), 887−898.

(57) Menegatti, R.; Cunha, A. C.; Ferreira, V. F.; Perreira, E. F. R.; El-Nabawi, A.; Eldefrawi, A. T.; Albuquerque, E. X.; Neves, G.; Rates, S. M. K.; Fraga, C. A. M.; Barreiro, E. J. Design, synthesis and pharmacological profile of novel dopamine D$_2$ receptor ligands. *Bioorg. Med. Chem.* **2003**, *11* (22), 4807−4813.

(58) Chornous, V. A.; Bratenko, M. K.; Vovk, M. V. Synthesis of 1-aryl-4-formylpyrazoles from acetaldehyde N-aryl-hydrazones by the Vilsmeier-Haack method. *Chem. Heterocycl. Compnd.* **2006**, *42* (9), 1242−1243.

(59) Teodoro, O.; Silva, J.; Moutinho, A. M. C. Multitechnique Surface-Analysis System - Apparatus Description. *Vacuum* **1995**, *46* (8−10), 1205−1209.

(60) Payne, B. P.; Biesinger, M. C.; McIntyre, N. S. X-ray photoelectron spectroscopy studies of reactions on chromium metal and chromium oxide surfaces. *J. Elect. Spec. Rel. Phenom.* **2011**, *184* (1−2), 29−37.